

# Protective Polymer Coatings for High-Throughput, High-Purity Cellular Isolation

Gabriela Romero,<sup>†,‡</sup> Jacob J. Lilly,<sup>†</sup> Nathan S. Abraham,<sup>§</sup> Hainsworth Y. Shin,<sup>⊥</sup> Vivek Balasubramaniam,<sup>||</sup> Tadahide Izumi,<sup>#</sup> and Brad J. Berron<sup>\*,†</sup>

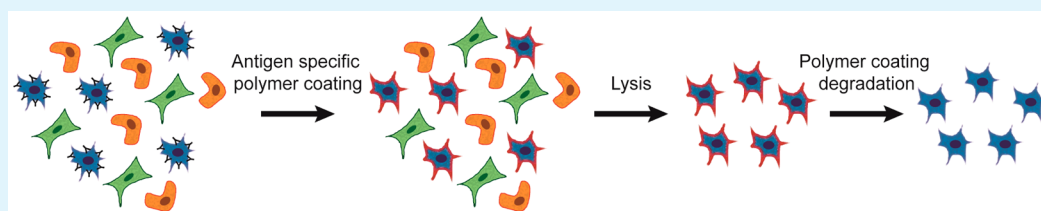
<sup>†</sup>Department of Chemical and Materials Engineering, <sup>⊥</sup>Department of Biomedical Engineering, University of Kentucky, Lexington, Kentucky 40506, United States

<sup>§</sup>Department of Chemical Engineering, University of Massachusetts Amherst, Amherst, Massachusetts 01003, United States

<sup>||</sup>Department of Pediatrics, University of Wisconsin, Madison, Wisconsin 53792, United States

<sup>#</sup>Graduate Center for Toxicology, University of Kentucky, Lexington, Kentucky 40536, United States

## S Supporting Information



**ABSTRACT:** Cell-based therapies are emerging as the next frontier of medicine, offering a plausible path forward in the treatment of many devastating diseases. Critically, current methods for antigen positive cell sorting lack a high throughput method for delivering ultrahigh purity populations, prohibiting the application of some cell-based therapies to widespread diseases. Here we show the first use of targeted, protective polymer coatings on cells for the high speed enrichment of cells. Individual, antigen-positive cells are coated with a biocompatible hydrogel which protects the cells from a surfactant solution, while uncoated cells are immediately lysed. After lysis, the polymer coating is removed through orthogonal photochemistry, and the isolate has >50% yield of viable cells and these cells proliferate at rates comparable to control cells. Minority cell populations are enriched from erythrocyte-depleted blood to >99% purity, whereas the entire batch process requires 1 h and <\$2000 in equipment. Batch scale-up is only contingent on irradiation area for the coating photopolymerization, as surfactant-based lysis can be easily achieved on any scale.

**KEYWORDS:** cell isolation, photopolymerization, polymer, coatings, protein expression, sorting

Increasingly, clinicians and researchers are seeking to use differentiated cells from a patient's own stem cells to replenish a damaged cell population and naturally restore biological function.<sup>1,2</sup> A major barrier to this regenerative therapy is the unintended transplantation of undifferentiated cells which have a high risk for tumor formation.<sup>3</sup> As such, high purity sorting for lineage-positive populations from the undifferentiated cells is a high priority in clinical applications. This purity requirement becomes even more challenging when considering the enormous quantities of cells used in these applications. As an extreme example, loading differentiated cells into a decellularized rat liver uses  $10^8$  purified cells,<sup>4</sup> which translates to roughly  $10^{10}$  cells for human application. Similar size scale and purity arguments can be made for the use of islet cells to treat diabetes,<sup>5</sup> chondrocytes to regenerate cartilage,<sup>6</sup> and endothelial progenitor cells for tissue repair following an ischemic event.<sup>7</sup>

Researchers currently have a portfolio of technologies to meet many of their cell sorting needs. Critically, there is a technology gap in isolating lineage-positive cells from undifferentiated lineage-negative cells in a rapid, highly pure

manner. Magnetic sorting excels in high-speed, low-cost sorting, but is hampered in purity by nonspecific adsorption in antigen-positive sorts.<sup>8</sup> Fluorescence-activated cellular sorting (FACS) delivers exceptional purity but at low throughput and high cost.<sup>9</sup> Microfluidic approaches are promising, but purities for populations adhered to antibody-coated surfaces is typically low (<50%),<sup>10</sup> throughput is limited (~10 mL or  $1 \times 10^8$  cells per day),<sup>11</sup> and recovery of isolated cells from the devices has proven difficult.<sup>12</sup> The most common approach for sorting large numbers of antigen positive cells at high purity is a sequential approach where cells are enriched with magnetic sorting, and purity is attained with FACS.<sup>13</sup> Even in this debulked case, each antigen-positive cell must pass through a FACS system, and throughput for high purity sorts is typically  $\sim 1 \times 10^7$  cells/day, involving time-consuming sterilization and gate adjustment operations. The stark contrast

Received: July 13, 2015

Accepted: August 5, 2015

Published: August 5, 2015

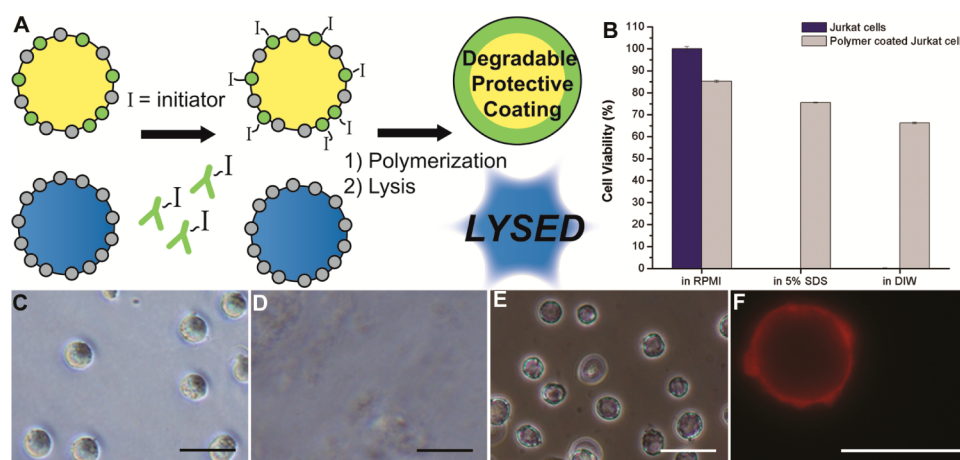


**Figure 1.** Pure populations of marker-positive cells through polymerization. (A) Cells are immunolabeled with polymerization initiators, and protective coatings are formed only on initiator labeled cells. Unprotected cells are lysed while coated cells are viable. (B) Calcein viability assay of Jurkat cells and polymer-coated Jurkat cells after 10 min in indicated solution. Data are mean  $\pm$  s.d. (C) Naive Jurkat cells. (D) Uncoated Jurkat cells are lysed in <10 s in 5% SDS. Only sparse cellular debris remains in the viscous lysate. (E) Polymer-coated Jurkats intact are after 10 min in 5% SDS. (F) Epifluorescent image of Jurkat cells coated with a red fluorescent nanoparticle-loaded polymer in pure deionized water. Scale bars are 25  $\mu$ m.

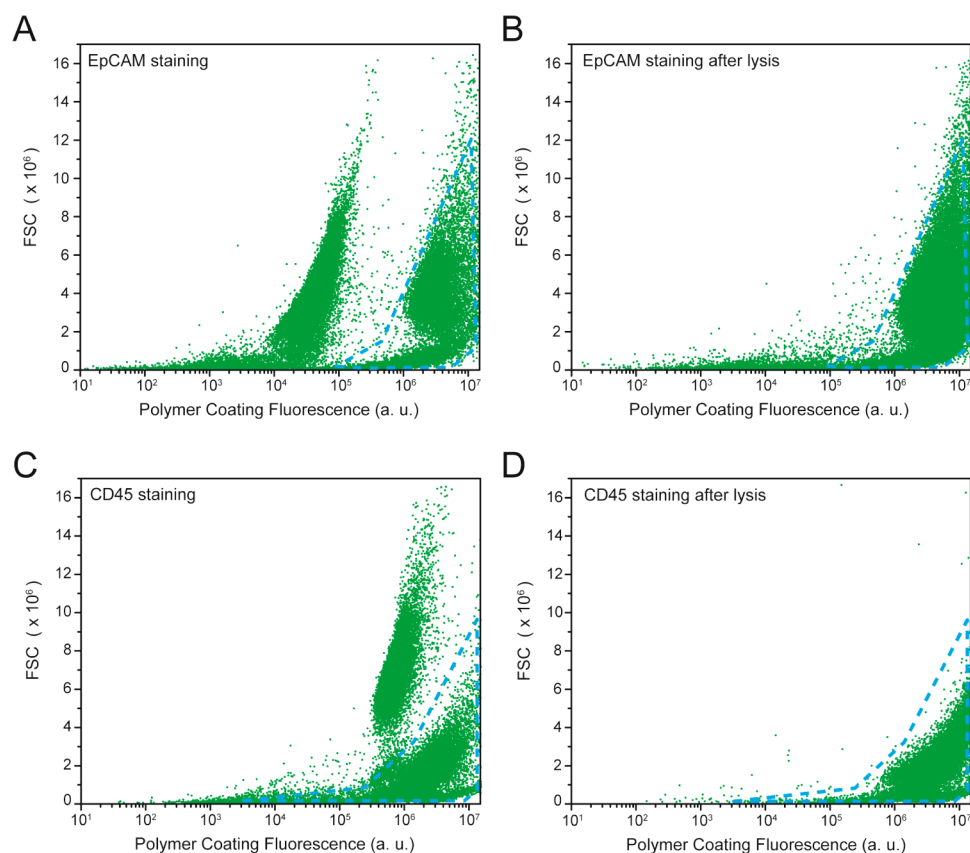


**Figure 2.** Specific lysis of cultured cells. Representative flow cytometric analysis of populations before and after exposure to SDS. (A) Coating targeted to EpCAM+ cells from an initial population of 8% A549 and 90% Jurkat after polymerization. (B) Population from A after 5 min exposure to 5% SDS. (C) Coating targeted to CD45+ cells from an initial population of 9% Jurkat and 91% A549 after polymerization. (D) Population from C after 5 min exposure to 5% SDS.

in magnitude between rates achievable with FACS and the requirements of regenerative medicine illustrates a critical obstacle in the future of these revolutionary treatment modalities.

Here, we present a fundamentally new approach to cellular sorting. Antigen-specific lysis (ASL) consists of specific cellular protection by a temporary polymer coating and the subsequent

lysis of unprotected cells (Figure 1A). The formation of a polymer film requires a polymerization initiator,<sup>14</sup> and ASL utilizes antibodies to localize eosin (a type II photoinitiator) on the surface of only antigen-positive cells.<sup>15–17</sup> Coatings are formed upon immersion in nitrogen-purged monomer mix (25 wt % UV cleavable PEG diacrylate,<sup>18</sup> 21 mM triethanol amine, 35 mM 1-vinyl-2-pyrrolidinone, and 0.05 wt % fluorescent

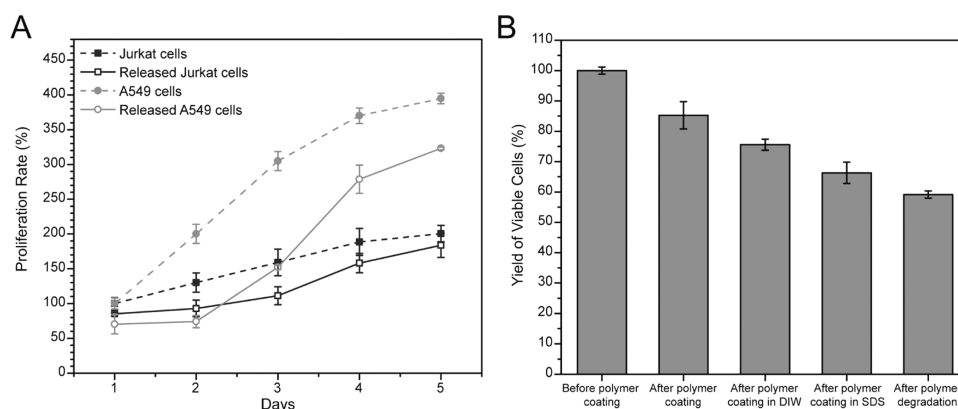


**Figure 3.** Proliferation and viability of processed cells. (A) Proliferation rates of naive (dashed line) or processed/released (solid line) cells. Jurkat cells (blue). A549 cells (gray). (B) Viability of Jurkat cells at critical steps in antigen specific lysis processing. Data are mean  $\pm$  s.d.

nanoparticles in 1 $\times$  phosphate buffer) and 530 nm LED irradiation (30 mW/cm<sup>2</sup>) for 10 min, where a red fluorescent polymer coating is formed on the outside of only targeted, initiator-labeled cells. When the photoinitiators are targeted against protein tyrosine phosphatase (CD45 antigen), protective polymer coatings are formed on the outside of Jurkat cells.<sup>16,19</sup> Unprotected mammalian cells (Figure 1C) are lysed and killed by a 10 min exposure to 5% SDS (Figure 1D),<sup>20</sup> where we observe cells encapsulated fluorescent coatings which retain both cellular integrity and activity. Cellular integrity was determined visually (Figure 1E) and by SYTOX assay (>80% viable in Figure S1). Viability by cellular activity was determined by calcein esterase activity assay (>80% in Figure 1B) and by lack of activation of caspase-3/7 apoptotic pathways (<5% apoptotic in Figure S1). This cellular protection by a targeted coating is the foundation of ASL sorting, where complete elimination of the untargeted population is feasible through conventional approaches of cell lysis. Although enrichment based on the exclusion of SDS is a chemical means of selection, we have also demonstrated the preservation of cellular function in hypotonic solutions using similar coatings. Immersion of 1  $\times$  10<sup>5</sup> uncoated Jurkat cells in 1 mL of pure water results in a large imbalance of salt concentration, leading to swelling and rupture of the cell.<sup>21</sup> When Jurkat cells are coated with a PEG diacrylate polymer, the polymer coating preserves cell membrane integrity and enzymatic function (Figure 1B, F).

In each mode of lysis, we have observed reductions in the numbers of uncoated cells within a population to undetectable (SDS lysis) or statistically insignificant levels (hypotonic lysis,  $p = 0.0517$ ), demonstrating the potential for ASL to deliver 100% pure populations with SDS or hypotonic lysis. We hypothesized that 5% SDS solution is excluded from the polymer coating because of the polymer mesh size ( $\sim 2.5$  nm),<sup>22</sup> which is a hundred times smaller than SDS micelles. At 5% SDS concentration (173.4 mM > CMC of 8 mM),<sup>23</sup> most of the surfactant is arranged into micelles, and the small fraction of free SDS molecules are either excluded by the hydrophobic interactions or penetrate through the polymer coating but the concentration is not high enough to disrupt the cell membrane. The limiting factor for ASL purity is the specificity of polymerization afforded by the antibody-targeted initiator species. To investigate the specificity of these polymer coatings, we isolated A549 cells from a mixed population with Jurkat cells. 10<sup>4</sup> A549 cells were added to 10<sup>5</sup> Jurkat cells. For the sake

of adaptability, we synthesized a streptavidin-eosin conjugate that can be targeted to A549 cells through the use of biotinylated antibodies against epithelial cell adhesion molecule antigen (anti-EpCAM). The cell mixture was labeled with initiator through incubation in 1:100 mouse anti-EpCAM for 40 min in a solution of 3% FBS in 1 $\times$  PBS, 1:200 biotinylated antimouse secondary, and then incubation in 10  $\mu$ g/mL streptavidin-eosin for 30 min. After polymerization (as before), the mixture of cells were analyzed by flow cytometry, and two distinct populations are observed that are consistent with control populations of coated A549 cells and naive Jurkat cells. The fraction of each gated population (8% A549 to 90% Jurkat, Figure 2A) is consistent with the fraction of starting populations. Upon addition of 5% SDS in PBS to the pelleted cellular mixture, a purified population of coated A549 cells is obtained through centrifugation (0.3g for 5 min) and rinsing in 3% FBS in PBS. Flow cytometry shows >98% of the population to be consistent with coated A549 cells (Figure 2B). Purity was further supported by fluorescence analysis of sorting a GFP-transfected A549 cell line. ASL was performed in cell mixtures of Jurkat cells and GFP-positive A549 cells, where isolated fraction consisted of 97.1  $\pm$  2.3% GFP-positive A549 cells, and 2.9  $\pm$  2.3% per each 10<sup>4</sup> cell batch were GFP-negative cells (Figure S2). A similar experiment to isolate minority Jurkat cells from A549 cells (9:91, respectively) using anti-CD45 to target the coatings yielded a > 96% pure Jurkat population by flow cytometry (Figure 2C, D).

Removal of the polymer coating is essential for translation of ASL as a cell isolation technology. We use a UV-degradable PEG-diacrylate monomer developed by Kloxin et al.<sup>18</sup> to temporally control the presence of the cross-linked polymer coating. Coated Jurkat cells were released from the polymer coating through 10 min exposure to 10 mW/cm<sup>2</sup>, 365 nm light in PBS and 10 mM EDTA. As photobleaching and particle release possibilities weaken the certainty of direct observation of coating removal by fluorescent means, the removal of the coatings was confirmed by proliferation assays of the released cells and comparison to naive Jurkat cell. While unreleased cells will die over a few days (Figure S3), the released Jurkat cells proliferate at rates comparable to naive Jurkat cells (Figure 3A). We also evaluated the proliferation of released A549 cells, which are anchorage dependent. The A549 cells had a 2 day lag in proliferation. Discrepancies between the anchorage dependent A549 and the anchorage independent Jurkat cells suggests residual polymer may interfere with critical cell–substrate

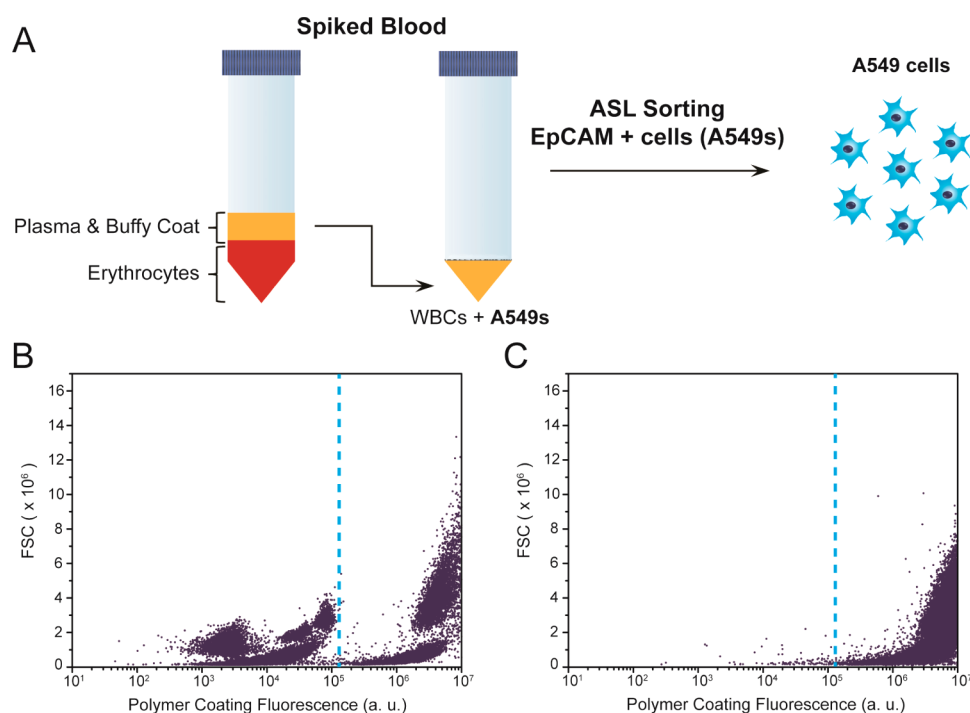


**Figure 4.** Isolation of EpCAM+ cells spiked into blood. (A) Overview of approach. (B) Flow cytometric data of A549 cell spiked into erythrocyte-depleted blood after EpCAM-specific polymerization. Dashed line indicates distinction between polymer coated A549 cells and other blood components based on control studies of pure populations. (C) Flow cytometric data after lysis of EpCAM- components.

interactions. Observation of the cells in culture showed viable cell spreading and residual red fluorescent polymer remaining after 1 day (Figure S4). PEG hydrogels have been commonly used to prevent cell–substrate interactions, and the screening of these interactions by residual polymer highlights an opportunity for improvement of ASL through the more efficient removal of the polymer coating. Yield of viable cells (>50% by calcein, Figure 3B) throughout the ASL process is comparable to FACS,<sup>9</sup> which is promising for a newly discovered technology. Viability was further supported by SYTOX (>70%) and apoptotic activity was detected in <5% of the released cells. There is a small (<10%) impact of UV light on cell viability by calcein (Figure S5) and negligible DNA damage as quantified by  $\gamma$  H2AX foci<sup>24–26</sup> (Figure S6).

To support the generalized use of ASL for isolations beyond cultured cells, we spiked A549 cells into the leukocyte-enriched plasma fraction harvested from human blood subjected to 1xg red cell sedimentation (Figure 4A). The mixed population was labeled with anti-EpCAM, biotin-anti-Mouse IgG, and streptavidin-eosin, prior to polymerization in the monomer formulation with 530 nm light at 30 mW/cm<sup>2</sup> for 10 min. The polymer coated A549 cells are distinguished from blood components by flow cytometry, constituting 16% of the nucleated cells in the mixture (Figure 4B). After exposure to 5% SDS, > 99% of nucleated cells remaining correspond with A549 cells as quantified by flow cytometry (Figure 4C). The scale-up of ASL promises the rapid processing of large quantities of cells. By starting with a large sample, rare populations may be isolated in appreciable numbers, allowing occult phenotypes to be studied beyond single-cell analytical techniques.

ASL constitutes a completely unique approach for cellular isolation. Even at this early stage in development, the potential is clear for a high-purity, high-viability cell isolation technique

for both small and large batch isolations. As in the popular antibody-coated microfluidic systems, ASL is limited to single antigen sorts at a given sensitivity. As such, it provides a high throughput alternative to microfluidic sorting which complements existing antigen-negative magnetic sorting technology for high throughput, high purity applications. Prior work has also shown the ease of tuning the sensitivity of antibody-directed polymer coating system through antibody dilution or competitive binding with nonlabeled probes.<sup>27</sup> As in all antibody-based sorting systems, ASL has the potential of inadvertently activating cells, and caution is advised when using this or another antibody-based system with easily activated cells prior to use. ASL's reliance on common light sources (LEDs from epifluorescent microscopes) allows capital costs to be >100 $\times$  cheaper than a FACS system. Furthermore, all ASL processing can be performed in common disposable labware, eliminating the expensive and time-consuming sterilization procedures used in most other sorting techniques. Additionally, others have shown fluorescein to be a reasonable alternative to eosin-based initiation, where FITC-labeled antibodies could potentially replace our custom eosin conjugates.<sup>28</sup> Further developments using fluorescein-antibody conjugates for polymerization initiators would logically make ASL even more accessible to a broad range of researchers.

## ■ ASSOCIATED CONTENT

### 📄 Supporting Information

The Supporting Information is available free of charge on the ACS Publications website at DOI: 10.1021/acsami.5b06298.

Experimental methods, detailed results about cell viability and toxicity, proliferation, cell identity, and experimental setup (PDF)



## ■ AUTHOR INFORMATION

## Corresponding Author

\*E-mail: brad.berron@uky.edu.

## Present Address

‡G.R. is currently at Vindico Pharmaceuticals Inc., Lexington, Kentucky 40506.

## Author Contributions

The manuscript was written through contributions of all authors. All authors have given approval to the final version of the manuscript.

## Funding

This work was supported partially by NIH R21 EB012188 and R01 HL127682–01. This work was supported partially by the National Science Foundation under Awards CBET-1351531 and EEC-0851716. The authors acknowledge the financial support from the National Cancer Institute (NCI) Grant R25CA153954 and a National Cancer Institute Cancer Nanotechnology Training Center (NCI-CNTC) Traineeship awarded to J.L.L. The views expressed in this manuscript do not represent the views of the NCI, NIH, NSF, or any other government agency or official.

## Notes

The authors declare no competing financial interest.

## ■ REFERENCES

(1) Amabile, G.; Meissner, A. Induced pluripotent stem cells: current progress and potential for regenerative medicine. *Trends Mol. Med.* **2009**, *15* (2), 59–68.

(2) Wu, S. M.; Hochedlinger, K. Harnessing the potential of induced pluripotent stem cells for regenerative medicine. *Nat. Cell Biol.* **2011**, *13* (5), 497–505.

(3) Fong, C.-Y.; Gauthaman, K.; Bongso, A. Teratomas from pluripotent stem cells: A clinical hurdle. *J. Cell. Biochem.* **2010**, *111* (4), 769–781.

(4) Uygun, B. E.; Soto-Gutierrez, A.; Yagi, H.; Izamis, M.-L.; Guzzardi, M. A.; Shulman, C.; Milwid, J.; Kobayashi, N.; Tilles, A.; Berthiaume, F. Organ reengineering through development of a transplantable recellularized liver graft using decellularized liver matrix. *Nat. Med.* **2010**, *16* (7), 814–820.

(5) Lin, C. C.; Anseth, K. S. Cell-cell communication mimicry with poly(ethylene glycol) hydrogels for enhancing beta-cell function. *Proc. Natl. Acad. Sci. U. S. A.* **2011**, *108* (16), 6380–6385.

(6) Brittberg, M.; Lindahl, A.; Nilsson, A.; Ohlsson, C.; Isaksson, O.; Peterson, L. Treatment of Deep Cartilage Defects in the Knee with Autologous Chondrocyte Transplantation. *N. Engl. J. Med.* **1994**, *331* (14), 889–895.

(7) Asahara, T.; Kawamoto, A.; Masuda, H. Concise Review: Circulating Endothelial Progenitor Cells for Vascular Medicine. *Stem Cells* **2011**, *29* (11), 1650–1655.

(8) Chalmers, J. J.; Xiong, Y.; Jin, X.; Shao, M.; Tong, X.; Farag, S.; Zborowski, M. Quantification of non-specific binding of magnetic micro- and nanoparticles using cell tracking velocimetry: Implication for magnetic cell separation and detection. *Biotechnol. Bioeng.* **2010**, *105* (6), 1078–1093.

(9) Arnold, L. W.; Lannigan, J. Practical Issues in High-Speed Cell Sorting. *Current Protocols in Cytometry* **2010**, 1.24. 1–1.24.30.

(10) Yu, M.; Stott, S.; Toner, M.; Maheswaran, S.; Haber, D. A. Circulating tumor cells: approaches to isolation and characterization. *J. Cell Biol.* **2011**, *192* (3), 373–382.

(11) Stott, S. L.; Hsu, C.-H.; Tsukrov, D. I.; Yu, M.; Miyamoto, D. T.; Waltman, B. A.; Rothenberg, S. M.; Shah, A. M.; Smas, M. E.; Korir, G. K.; Floyd, F. P., Jr.; Gilman, A. J.; Lord, J. B.; Winokur, D.; Springer, S.; Irimia, D.; Nagrath, S.; Sequist, L. V.; Lee, R. J.; Isselbacher, K. J.; Maheswaran, S.; Haber, D. A.; Toner, M. Isolation of

circulating tumor cells using a microvortex-generating herringbone-chip. *Proc. Natl. Acad. Sci. U. S. A.* **2010**, *107* (43), 18392–18397.

(12) Shah, A. M.; Yu, M.; Nakamura, Z.; Ciciliano, J.; Ulman, M.; Kotz, K.; Stott, S. L.; Maheswaran, S.; Haber, D. A.; Toner, M. Biopolymer System for Cell Recovery from Microfluidic Cell Capture Devices. *Anal. Chem.* **2012**, *84* (8), 3682–3688.

(13) Geens, M.; Van de Velde, H.; De Block, G.; Goossens, E.; Van Steirteghem, A.; Tournaye, H. The efficiency of magnetic-activated cell sorting and fluorescence-activated cell sorting in the decontamination of testicular cell suspensions in cancer patients. *Hum. Reprod.* **2007**, *22* (3), 733–742.

(14) Berron, B. J.; May, A. M.; Zheng, Z.; Balasubramaniam, V.; Bowman, C. N. Antigen-Responsive, Microfluidic Valves for Single Use Diagnostics. *Lab Chip* **2012**, *12* (4), 708–710.

(15) Avens, H. J.; Berron, B. J.; May, A. M.; Voigt, K. R.; Seedorf, G. J.; Balasubramaniam, V.; Bowman, C. N. Sensitive Immunofluorescent Staining of Cells via Generation of Fluorescent Nanoscale Polymer Films in Response to Biorecognition. *J. Histochem. Cytochem.* **2011**, *59* (1), 76–87.

(16) Avens, H. J.; Chang, E. L.; May, A. M.; Berron, B. J.; Seedorf, G. J.; Balasubramaniam, V.; Bowman, C. N. Fluorescent polymeric nanocomposite films generated by surface-mediated photoinitiation of polymerization. *J. Nanopart. Res.* **2011**, *13* (1), 331–346.

(17) Lilly, J. L.; Sheldon, P. R.; Hoversten, L. J.; Romero, G.; Balasubramaniam, V.; Berron, B. J. Interfacial Polymerization for Colorimetric Labeling of Protein Expression in Cells. *PLoS One* **2014**, *9* (12), e115630.

(18) Kloxin, A. M.; Kasko, A. M.; Salinas, C. N.; Anseth, K. S. Photodegradable Hydrogels for Dynamic Tuning of Physical and Chemical Properties. *Science* **2009**, *324*, 59.

(19) Lilly, J. L.; Romero, G.; Xu, W.; Shin, H. Y.; Berron, B. J. Characterization of Molecular Transport in Ultrathin Hydrogel Coatings for Cellular Immunoprotection. *Biomacromolecules* **2015**, *16*, 541.

(20) Brown, R. B.; Audet, J. Current techniques for single-cell lysis. *J. R. Soc., Interface* **2008**, *5* (Suppl 2), S131–S138.

(21) Harrison, R. G.; Todd, P.; Rudge, S. R.; Petrides, D. P. *Bioseparations Science and Engineering*; Oxford University Press: New York, 2003.

(22) Lilly, J. L.; Romero, G.; Xu, W.; Shin, H. Y.; Berron, B. J. Characterization of Molecular Transport in Ultrathin Hydrogel Coatings for Cellular Immunoprotection. *Biomacromolecules* **2015**, *16* (2), 541–549.

(23) Chatterjee, A.; Moulik, S. P.; Sanyal, S. K.; Mishra, B. K.; Puri, P. M. Thermodynamics of Micelle Formation of Ionic Surfactants: A Critical Assessment for Sodium Dodecyl Sulfate, Cetyl Pyridinium Chloride and Dioctyl Sulfosuccinate (Na Salt) by Microcalorimetric, Conductometric, and Tensiometric Measurements. *J. Phys. Chem. B* **2001**, *105* (51), 12823–12831.

(24) Barzilai, A.; Yamamoto, K.-I. DNA damage responses to oxidative stress. *DNA Repair* **2004**, *3* (8–9), 1109–1115.

(25) Sedelnikova, O. A.; Pilch, D. R.; Redon, C.; Bonner, W. M. Histone H2AX in DNA damage and repair. *Cancer Biol. Ther.* **2003**, *2* (3), 233–235.

(26) Rogakou, E. P.; Pilch, D. R.; Orr, A. H.; Ivanova, V. S.; Bonner, W. M. DNA double-stranded breaks induce histone H2AX phosphorylation on serine 139. *J. Biol. Chem.* **1998**, *273* (10), 5858–5868.

(27) Hansen, R. R.; Avens, H. J.; Shenoy, R.; Bowman, C. N. Quantitative evaluation of oligonucleotide surface concentrations using polymerization-based amplification. *Anal. Bioanal. Chem.* **2008**, *392* (1–2), 167–175.

(28) Lee, J. K.; Heimer, B. W.; Sikes, H. D. Systematic Study of Fluorescein-Functionalized Macrophotoinitiators for Colorimetric Bioassays. *Biomacromolecules* **2012**, *13* (4), 1136–1143.